

**Matrix product states with backflow correlations**Guglielmo Lami<sup>1</sup>,<sup>✉</sup> Giuseppe Carleo,<sup>2</sup> and Mario Collura<sup>1</sup><sup>✉</sup><sup>1</sup>*International School for Advanced Studies (SISSA), I-34136 Trieste, Italy*<sup>2</sup>*Ecole Polytechnique Fédérale de Lausanne (EPFL), Institute of Physics, CH-1015 Lausanne, Switzerland*

(Received 18 January 2022; revised 28 April 2022; accepted 31 May 2022; published 10 August 2022)

By taking inspiration from the backflow transformation for correlated systems, we introduce a tensor network *Ansatz* which extends the well-established matrix product state representation of a quantum many-body wave function. This structure provides enough resources to ensure that states in dimensions larger than or equal to one obey an area law for entanglement. It can be efficiently manipulated to address the ground-state search problem by means of an optimization scheme which mixes tensor-network and variational Monte Carlo algorithms. We benchmark the *Ansatz* against spin models both in one and two dimensions, demonstrating high accuracy and precision. We finally employ our approach to study the challenging  $S = 1/2$  two-dimensional (2D)  $J_1$ - $J_2$  model, demonstrating that it is competitive with the state-of-the-art methods in 2D.

DOI: [10.1103/PhysRevB.106.L081111](https://doi.org/10.1103/PhysRevB.106.L081111)

Understanding quantum many-body (QMB) systems in and out of equilibrium is one of the most exciting open challenges in physics. In recent years, significant progress has been made in the study of strongly correlated systems. Several experimental approaches implementing Feynman's simulators [1] are allowing the controlled exploration of uncharted territory [2–8].

On the theoretical level, the development of tensor-network (TN) techniques has significantly expanded the scope of variational approaches to QMB systems since the introduction of the density-matrix renormalization group (DMRG) algorithm [9]. The TN's goal is to represent the QMB wave functions by means of a set of tensors, connected in a generic network via auxiliary bonds with finite dimension, thus overcoming computational limitations due to the exponentially large Hilbert space [10,11]. The bond dimension  $\chi$  can be adjusted to manipulate the information content of the TN, thus going from product states ( $\chi = 1$ ), reproducing mean-field approximations, to the exact but inefficient wave-function representation. In one dimension (1D), the matrix product state (MPS) geometry has demonstrated an unprecedented accuracy for both equilibrium and out-of-equilibrium problems [12,13]. However, TNs have some fundamental limitations, such as the intrinsic hardness of finding efficient contraction schemes [14] and unfavorable scaling of the required resources with the system size in higher dimensions [10]. Most successful TN geometries, such as projected entangled pair states (PEPS) [15] and tree tensor networks [16], suffer from drawbacks: While the latter does not satisfy the entanglement area law (although some effort has been spent to overcome this limitation in Ref. [17]), the former suffer from high algorithmic complexity,  $O(\chi^{10})$ , and lack exact computation of expectation values.

In parallel to the progress of TNs, artificial neural networks (NNs) have been discovered and used in a plethora of scientific fields, proving astonishing versatility in physics

applications [18]. In recent years, they have been employed as a variational *Ansatz* for QMB problems [19]. In this context, a number of possible architectures have been tried, such as the restricted Boltzmann machine [19,20], feed-forward NN [21,22], and recurrent NN [23]. These *Ansätze* have been proven to have a great descriptive power [21,24]. However, the number of parameters entering a NN wave function may be large and the appropriate network structure is usually not clear *a priori*. Understanding an optimal geometry encoding information from the specific dimensionality and taking advantage from both TN and NN structures could be the ultimate solution to the QMB problem.

NNs are optimized with variational Monte Carlo (VMC) methods [25]. A key tool is the so-called automatic differentiation [26], which allows us to efficiently compute cost-function derivatives with machine precision. This paradigm has been recently applied also to TN optimization [27]. Combining such approaches with standard TN algorithms appears as a promising way to find strategies to solve open problems at the equilibrium and out of equilibrium. Efforts in this direction were made with the introduction of the entangled plaquette states (EPS) [28,29], Monte Carlo optimized PEPS [30], and infinite PEPS optimized with automatic differentiation [31]. The space of possible hybrid wave functions is however still largely unexplored. Here, we introduce a variational *Ansatz*, generalizing the usual MPS. The *Ansatz* is inspired by the so-called backflow technique, employed in electronic-structure theory [32–34]. These matrix product backflow states (MPBS) can overcome some limitations of MPS by encoding an extensive amount of entanglement and keeping the algorithmic complexity under control. We further introduce an optimization scheme mixing DMRG and VMC recipes which can be proficiently applied to MPBS in order to find QMB ground states. As a benchmark, we employ this approach against well-known 1D and 2D spin models. Finally, we simulate the  $J_1$ - $J_2$  model,

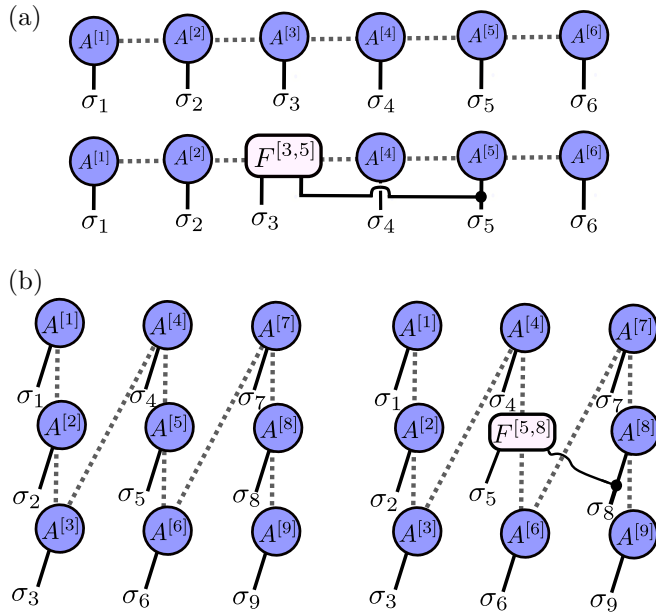


FIG. 1. Graphical representations of MPS and MPBS applied to (a) 1D and (b) 2D systems. The  $F$  tensors encode correlations between different lattice sites. The pictures represent only one of the terms in which  $F$  is involved (see Supplemental Material [36]).

providing the ability to inspect challenging highly nontrivial models.

*Matrix product backflow states.* A state  $|\psi\rangle$  of a QMB system consisting of  $N$  spin- $\frac{1}{2}$  variables is specified by the complex-valued function  $\psi(\sigma) = \langle \sigma | \psi \rangle$ ,  $\sigma \in \{\pm 1\}^N$  being the spin projections along the  $z$  direction. MPS [12] are defined by the functional form

$$\psi[A](\sigma) = A^{[1]}(\sigma_1)A^{[2]}(\sigma_2) \cdots A^{[N]}(\sigma_N), \quad (1)$$

where local tensors  $A^{[l]}(\sigma_i)$  have one physical index  $\sigma_i$  and two auxiliary indices. They can be graphically represented as three-legged shapes connected with lines, i.e., contracted along auxiliary indices (see Fig. 1) [12,35].

These indices run from 1 to a set of integers  $\chi_i$ , called bond dimensions, fixing the maximum amount of entanglement entropy (EE) which can be encoded by the state [12]. MPS provide good approximations of low-entangled states, as for instance ground states of local gapped Hamiltonians in 1D, for which an EE area law can be proven [37]. On the contrary, MPS cannot efficiently encode a volume law, since this requires an exponentially large value of  $\chi$ .

In order to overcome these limitations, we introduce a set of tensors  $F^{[i,j]}(\sigma_i, \sigma_j)$  with two physical indices  $\sigma_i, \sigma_j$  and two auxiliary indices. These will encode correlations between different lattice sites  $i, j$ . We propose a class of wave functions  $\psi[A, F](\sigma)$  obtained by replacing the MPS *local* tensors  $A^{[l]}(\sigma_i)$  as follows,

$$A^{[l]}(\sigma_i) \rightarrow A^{[l]}(\sigma_i) + \sum_{i_i \neq l} F^{[l, i_i]}(\sigma_i, \sigma_{i_i}), \quad (2)$$

which is explicitly depending on the *global* set of quantum numbers  $\sigma$ . This wave function can be considered conceptually similar to the well-known backflow wave function in

electronic structure theory, which is used to introduce correlations in the mean-field theory by taking the single-particle orbitals acting on configuration-dependent quasiparticle positions [32–34,38]. In our case, the starting point is not a mean-field wave function, but rather an MPS, which can be seen as a systematic improvement of the mean-field approximation. We thus refer to this class of variational states matrix product backflow states (MPBS). It is worth mentioning that MPBS wave functions admit a series expansion in increasing powers of  $F$ , where each term can be formally recast as an MPS with a locally larger bond dimension (up to  $2^n$  times the original bond dimension, at order  $n$ ). Examples of first-order terms are depicted in Fig. 1 [details in the Supplemental Material (SM) [36]]. MPBS with  $F$  connected as in Fig. 1(b) will be used below to simulate 2D systems. They satisfy an area law for EE, since *any* possible grid bipartition cuts a number of auxiliary bonds and/or  $F$  tensors that grow linearly with the length of the perimeter of the subsystem. Remarkably, it can be proven that the MPBS' ability to encode entanglement can be greater, since with a particular choice of the parameters one can encode a volume law for the EE (see SM [36]). Thus, MPBS can in principle provide good approximations not only of the ground states in 2D, but also of highly entangled states, as for instance time-evolved states after quantum quenches [39]. From an operative perspective, MPBS naturally suggest a two-step optimization algorithm: First, the local  $A$  tensors are optimized by using the usual MPS machineries; second, the nonlocal  $F$  tensors are optimized by means of VMC techniques. This alternated optimization approach has the advantage that the starting point of VMC optimization is not a random point in the parameter space, but rather an already acceptably good approximation of the QMB wave function. Moreover, VMC optimization can further optimize the  $A$  tensors as well, thus providing an unrestricted variational search for our *Ansatz* in the last optimization stage. Finally, the MPBS network can be exactly contracted during the Monte Carlo steps (in contrast to other similar approaches where approximated contraction schemes are employed [30]), leading to a purely variational scheme. In the following, we will focus on the ground-state search, benchmarking the MPBS *Ansatz* on both 1D and 2D models. The numerical results are obtained by means of the two-step optimization algorithm just outlined. The implementation was done in Python by means of NETKET [40–44], a package providing machine learning and automatic differentiation methods for QMB systems (see SM [36]).

*Modified Haldane-Shastry (HS) model.* First, we apply MPBS to a 1D spin chain with periodic boundary conditions. In particular, we consider the modified Haldane-Shastry (HS) model  $\mathcal{H}_{\text{HS}} = \sum_{j < i} (1/\tilde{d}_{ij})^2 (-\sigma_i^x \sigma_j^x - \sigma_i^y \sigma_j^y + \sigma_i^z \sigma_j^z)$ , where  $\tilde{d}_{ij} = (N/\pi) \sin(\pi/N|i-j|)$ . This model is known to be challenging for standard DMRG, as it shows power-law scaling in the ground-state EE [46]. To use our optimization scheme, we adapt the MPBS *Ansatz* in order to realize translational invariance. This is achieved by adding an extra auxiliary index, connecting the first and last site, and by taking the  $A$  tensors independent from the site  $i$ . Also, we set  $F^{[i,j]}$  to be dependent only on the distance  $d_{ij} = \min(|i-j|, N-|i-j|)$  between the connected sites. We also introduced a cutoff  $r_c$  setting the maximum distance between sites for which the  $F$  tensors are nonzero. Due to translational invariance and the

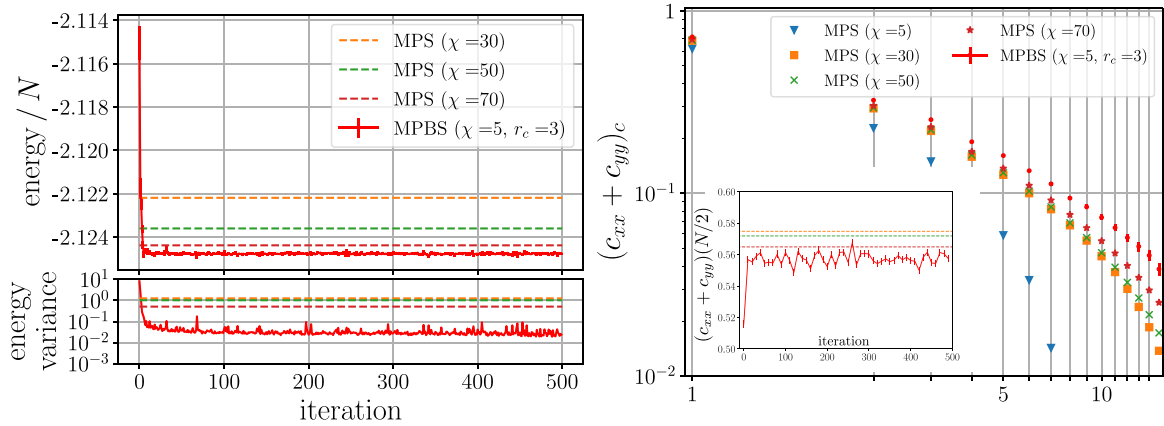


FIG. 2. MPBS of bond dimension  $\chi = 5$  tested with the modified 1D HS model: energy density convergence (left) and  $(c_{xx} + c_{yy})_c$  connected correlator (right). The system size is  $N = 70$ .

imposed cutoff, the number of variational parameters of the *Ansatz* is independent of the system size  $N$ , resulting in a reduced computational cost for the VMC simulation. In the first optimization stage, we write the Hamiltonian as a matrix product operator and use DMRG [12,47] to get the optimized  $A$  tensors. In the second stage, a VMC optimization of the  $F$  tensors is realized, adopting the stochastic-reconfiguration [48] approach. Since  $\mathcal{H}_{\text{HS}}$  commute with the total  $z$  magnetization  $\Sigma^z = \sum_{i=1}^N \sigma_i^z$  and parity  $P = \sigma_1^x \sigma_2^x \cdots \sigma_N^x$ , we restrict the ground-state search to the  $\Sigma^z = 0$  sector. Figure 2 shows selected results obtained with a relatively small value of the MPBS bond dimension ( $\chi = 5$ ) and  $r_c = 3$ . The first subplot shows the expectation value and variance of the energy, tracked during the VMC optimization. Dotted lines represent DMRG energies/variances for increasing values of the bond dimension. After  $<10^2$  VMC steps the MPBS energy reaches values smaller than the DMRG energy obtained with the larger value of  $\chi$  ( $\chi = 70$ ). Let us remark that the number of parameters of this MPS is much larger than the number of parameters of our *Ansatz*. The second subplot in Fig. 2 shows the two-point connected correlator  $(c_{xx} + c_{yy})_c$ , computed by taking the average of  $\langle \sigma_i^x \sigma_{i+r}^x \rangle + \langle \sigma_i^y \sigma_{i+r}^y \rangle$  over  $i$  and subtracting the square of the average  $x$  and  $y$  magnetizations. The red points represent estimations obtained at the end of the VMC optimization, whereas the other points are DMRG results. These seem to converge to VMC values when increasing the bond dimension. In the inset we show the correlator  $c_{xx}(N/2) + c_{yy}(N/2)$  estimated during the Monte Carlo iterations. The convergence appears to be fast. Other applications of the MPBS *Ansatz* to 1D systems are reported in SM [36].

*Two-dimensional Ising model.* To corroborate the flexibility of MPBS in describing higher-dimensional systems, we now start analyzing 2D QMB models living on a square lattice of size  $N_x \times N_y$  with open boundary conditions. A simple way to adapt MPS to the description of such a system is to order the sites of the grid following a one-dimensional “snaking” path connecting the sites [see Fig. 1(b)] [49]. Other 2D to 1D mappings have been studied [50], leading to increased numerical precision but not to a significant improvement in the codification of entanglement in 2D systems. The main issue is that, since the area law in 2D implies that EE grows linearly with the length of the subsystem perimeter, any MPS

cannot describe efficiently the typical ground states of 2D Hamiltonians. As a possible improvement, we propose to arrange the MPBS *Ansatz* in order to codify correlations between sites which are adjacent in the 2D geometry but which are placed at a distance  $N_y$  along the 1D snaking path. This can be done by setting the  $F^{[i]}(\sigma_i, \sigma_j)$  matrices different from zero in the cases in which  $j = i \pm N_y$ , where we label the lattice sites with a single integer  $i = 1, 2, \dots, N$ . As mentioned, an MPBS of this kind can encode the area law for the EE and, at least for a particular choice of the parameters, the volume law (see SM [36]). To benchmark the efficacy of MPBS in simulating 2D systems, we consider the Ising Hamiltonian  $\mathcal{H} = -\sum_{\langle i,j \rangle} \sigma_i^z \sigma_j^z + h \sum_i \sigma_i^x$  on a lattice of dimension  $N_x = N_y = 11$ . In Fig. 3, we show the results of an MPBS optimization, which was run with bond dimension  $\chi = 5$  and transverse field  $h = 3.0$ , close to the quantum critical point of the system  $h_c \simeq 3.044$  [51]. These results are compared with DMRG findings at different bond dimensions and with the energy value obtained by Lubasch and others by means of PEPS [45]. As in the previous case, MPBS with an extremely small bond dimension leads, after  $\approx 100$  VMC iterations, to results significantly better than DMRG, both in terms of energy density and variance. Since the system has rotational symmetry, during the last  $\simeq 150$  Monte Carlo iterations we explicitly symmetrize the MPBS with respect to the  $C_4$  group of fourfold rotations. We therefore consider the modified wave function  $\psi'[A, F](\sigma) = \sum_{k=0}^3 \psi[A, F](R^k \sigma)$ , where  $R$  is a rotation of  $\pi/2$  of the spin configuration. This results in a further improvement of the energy and energy variance. The value of the energy density we find at the end of the optimization is  $\langle \mathcal{H} \rangle / N = -3.17208(1)$ , in agreement with recent findings [23]. In the second subplot, we show the correlator  $c_{zz}(r) = \frac{1}{N_r} \sum_{r, |r|=r} \langle \sigma_{i_c}^z \sigma_{i_c+r}^z \rangle$ , where  $i_c$  indicates the central site of the grid and  $N_r$  is the number of sites placed at distance  $r$  from this. MPBS points seem to be in agreement with the trend of DMRG results for increasing bond dimension.

*Two-dimensional  $J_1$ - $J_2$  model.* Finally, we consider the antiferromagnetic  $J_1$ - $J_2$  model, with Hamiltonian  $\mathcal{H} = J_1 \sum_{\langle i,j \rangle} \sigma_i \cdot \sigma_j + J_2 \sum_{\langle\langle i,j \rangle\rangle} \sigma_i \cdot \sigma_j$ , where the first (second) sum is on first- (second-) nearest-neighbor couples of sites. This is a prototypical frustrated magnetic system. Despite active research in the past decades [52–55], the nature of

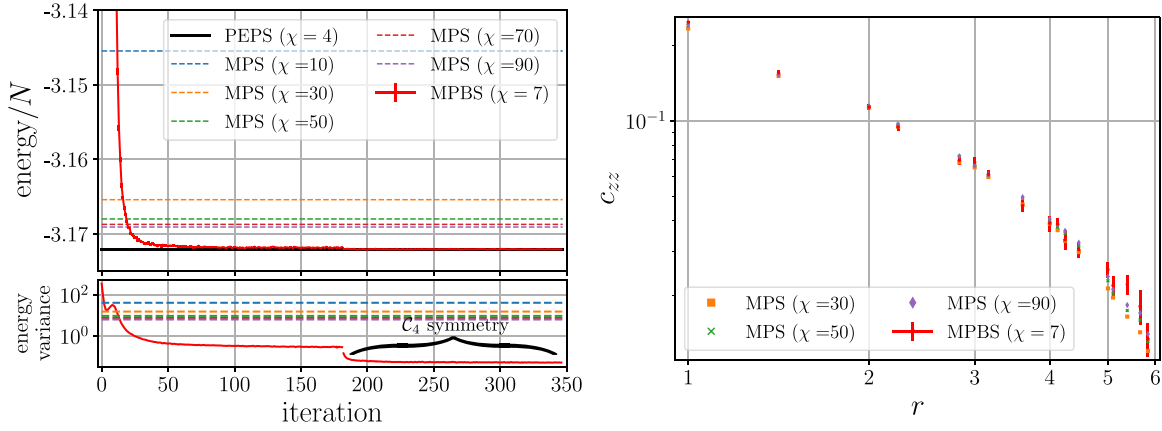


FIG. 3. MPBS of bond dimension  $\chi = 7$  tested with the 2D Ising model ( $N_x = 11, N_y = 11$ ): energy density convergence (left) and  $c_{zz}$  correlator (right). The PEPS result is taken from Ref. [45].

the ground state around the point of maximum frustration  $J_2/J_1 = 0.5$  remains unclear. We address the problem Hamiltonian by means of MPBS arranged as above and also adding  $F$  tensors connecting second-nearest-neighbor sites (see SM for details [36]). As in the HS model, we reduce the simulation to the zero magnetization sector. In Fig. 4 we show some selected results obtained with a system of size  $N_x = N_y = 8$  and  $J_1 = 1, J_2 = 0.5$ . After  $\simeq 350$  VMC optimization iterations, we apply  $C_4$  wave-function symmetrization. We compare our results with the EPS and PEPS results reported in Ref. [28] and with Monte Carlo optimized PEPS results reported in Ref. [55]. The final energy density of our simulation is  $\langle \mathcal{H} \rangle / N = -1.9273(9)$  and is lower than both values reported in Ref. [28], whereas it is about  $\approx 7 \times 10^{-3}$  greater than the value reported in Ref. [55]. It should be however remarked that the value in Ref. [55] is not strictly variational, because of the approximate contraction scheme adopted for PEPS. Finally, we measure relevant observables as the correlators  $c_{\text{ver}}(r) = \frac{1}{N_x} \sum_j \langle \sigma_{1,j} \cdot \sigma_{1+r,j} \rangle$  and  $c_{\text{hor}}(r) = \frac{1}{N_y} \sum_i \langle \sigma_{i,1} \cdot \sigma_{i,1+r} \rangle$ , which are shown in the second half of Fig. 4. These are respectively the average spin-spin correlators along the columns and the rows of the grid. Since the wave function  $\psi[A, F](\sigma)$  is symmetric under a rotation of  $\pi/2$ ,

we always find values for these correlators to be compatible within the uncertainty bars. On the contrary, DMRG results show that MPS are unable to encode power-law decaying correlations along the horizontal direction. We also measure the structure factor  $S^2(\mathbf{q}) = \frac{1}{[N(N+2)]} \sum_{i,j} \langle \sigma_i \cdot \sigma_j \rangle e^{-i\mathbf{q} \cdot (i-j)}$  for different pitch vectors  $\mathbf{q}$ . We find  $S^2(0, \pi) \simeq 3.19(5) \times 10^{-2}$  and  $S^2(\pi, \pi) \simeq 0.241(3)$ . The latter corresponds to the Néel order parameter. Both values are compatible with similar findings in Ref. [54]. We also obtain  $S^2(0, 0) = 1.3(2) \times 10^{-4}$ , consistent with the expectation that the  $J_1$ - $J_2$  ground state is in a singlet under  $SU(2)$  global symmetry.

*Conclusions and outlook.* We have introduced a variational Ansatz which exploits state-of-the-art numerical techniques based on tensor networks and automatically differentiable variational Monte Carlo. This many-body wave function encodes area law entanglement for high-dimensional systems. The efficiency of MPBS allows us to study challenging 2D models, encoding accurate long-range correlations and going beyond the *standard* PEPS and MPS Ansätze. The MPBS structure takes its root from the usual MPS, whose descriptive power is augmented by introducing a class of long-ranged tensors. This arranged network is well suited for a two-step optimization scheme, i.e., DMRG followed by VMC. The

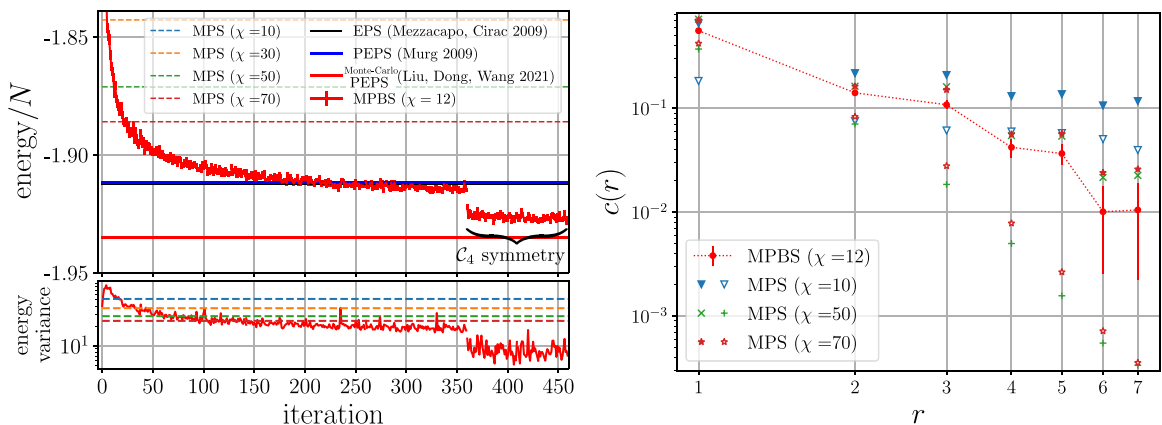


FIG. 4. MPBS of bond dimension  $\chi = 12$  tested with the  $J_1$ - $J_2$  model on a square lattice ( $N_x = 8, N_y = 8$ ). PEPS and EPS results are taken from Ref. [28]. In the right plot, solid (open) markers represent DMRG results for  $c_{\text{ver}}(r)$  [ $c_{\text{hor}}(r)$ ], and red points are MPBS results.

second step takes advantages from using an already reasonably good initialization of the QMB wave function and also to the use of an exact contraction scheme. The results presented in this Letter regarding well-known models, such as the 1D and 2D Ising model and 1D Haldane-Shastry model, provide evidence that MPBS constitutes a good *Ansatz* to approximate the ground states of QMB systems in 1D and 2D, via a purely

variational approach. It can also be employed to study highly nontrivial systems, such as the 2D  $J_1$ - $J_2$  frustrated model. The final optimized wave function can be easily used to compute useful observables. Significantly, the outlined two-step method can be applied also to the real-time dynamics problems. In this case, the time-dependent variational principle [56] followed by the time-dependent VMC can be used.

- 
- [1] R. Feynman, Simulating physics with computers, *Int. J. Theor. Phys.* **21**, 467 (1982).
- [2] P. Schauß, M. Cheneau, M. Endres, T. Fukuhara, S. Hild, A. Omran, T. Pohl, C. Gross, S. Kuhr, and I. Bloch, Observation of spatially ordered structures in a two-dimensional Rydberg gas, *Nature (London)* **491**, 87 (2012).
- [3] H. Labuhn, D. Barredo, S. Ravets, S. de Léséleuc, T. Macrì, T. Lahaye, and A. Browaeys, Tunable two-dimensional arrays of single Rydberg atoms for realizing quantum Ising models, *Nature (London)* **534**, 667 (2016).
- [4] H. Bernien, S. Schwartz, A. Keesling, H. Levine, A. Omran, H. Pichler, S. Choi, A. S. Zibrov, M. Endres, M. Greiner, V. Vuletić, and M. D. Lukin, Probing many-body dynamics on a 51-atom quantum simulator, *Nature (London)* **551**, 579 (2017).
- [5] P. Schauss, Quantum simulation of transverse Ising models with Rydberg atoms, *Quantum Sci. Technol.* **3**, 023001 (2018).
- [6] A. Omran, H. Levine, A. Keesling, G. Semeghini, T. T. Wang, and S. Ebadi, H. Bernien, A. S. Zibrov, H. Pichler, S. Choi, J. Cui, M. Rossignolo, P. Rembold, S. Montangero, T. Calarco, M. Endres, M. Greiner, V. Vuletić, and M. D. Lukin, Generation and manipulation of Schrödinger cat states in Rydberg atom arrays, *Science* **365**, 570 (2019).
- [7] I. Bloch, J. Dalibard, and W. Zwerger, Many-body physics with ultracold gases, *Rev. Mod. Phys.* **80**, 885 (2008).
- [8] F. Schäfer, T. Fukuhara, S. Sugawa, Y. Takasu, and Y. Takahashi, Tools for quantum simulation with ultracold atoms in optical lattices, *Nat. Rev. Phys.* **2**, 411 (2020).
- [9] S. R. White, Density Matrix Formulation for Quantum Renormalization Groups, *Phys. Rev. Lett.* **69**, 2863 (1992).
- [10] P. Silvi, F. Tschirsich, M. Gerster, J. Jünemann, D. Jaschke, M. Rizzi, and S. Montangero, The tensor networks anthology: Simulation techniques for many-body quantum lattice systems, *SciPost Phys. Lect. Notes* **8**, 41 (2019).
- [11] S. J. Ran, E. Tiritto, C. Peng, X. Chen, L. Tagliacozzo, G. Su, and M. Lewenstein, *Tensor Network Contractions*, Lecture Notes in Physics Vol. 964 (Springer, Berlin, 2020).
- [12] U. Schollwöck, The density-matrix renormalization group in the age of matrix product states, *Ann. Phys.* **326**, 96 (2011).
- [13] S. Paeckel, T. Köhler, A. Swoboda, S. R. Manmana, U. Schollwöck, and C. Hubig, Time-evolution methods for matrix-product states, *Ann. Phys.* **411**, 167998 (2019).
- [14] M. Kliesch, D. Gross, and J. Eisert, Matrix-Product Operators and States: NP-hardness and Undecidability, *Phys. Rev. Lett.* **113**, 160503 (2014).
- [15] F. Verstraete and J. I. Cirac, Renormalization algorithms for quantum-many body systems in two and higher dimensions, [arXiv:cond-mat/0407066](https://arxiv.org/abs/cond-mat/0407066).
- [16] Y.-Y. Shi, L.-M. Duan, and G. Vidal, Classical simulation of quantum many-body systems with a tree tensor network, *Phys. Rev. A* **74**, 022320 (2006).
- [17] T. Felser, S. Notarnicola, and S. Montangero, Efficient Tensor Network *Ansatz* for High-Dimensional Quantum Many-Body Problems, *Phys. Rev. Lett.* **126**, 170603 (2021).
- [18] G. Carleo, I. Cirac, K. Cranmer, L. Daudet, M. Schuld, N. Tishby, L. Vogt-Maranto, and L. Zdeborová, Machine learning and the physical sciences, *Rev. Mod. Phys.* **91**, 045002 (2019).
- [19] G. Carleo and M. Troyer, Solving the quantum many-body problem with artificial neural networks, *Science* **355**, 602 (2017).
- [20] R. G. Melko, G. Carleo, J. Carrasquilla, and J. I. Cirac, Restricted Boltzmann machines in quantum physics, *Nat. Phys.* **15**, 887 (2019).
- [21] O. Sharir, A. Shashua, and G. Carleo, Neural tensor contractions and the expressive power of deep neural quantum states, [arXiv:2103.10293](https://arxiv.org/abs/2103.10293).
- [22] G. Carleo, Y. Nomura, and M. Imada, Constructing exact representations of quantum many-body systems with deep neural networks, *Nat. Commun.* **9**, 5322(2018).
- [23] M. Hibat-Allah, M. Ganahl, Lauren E. Hayward, R. G. Melko, and J. Carrasquilla, Recurrent neural network wave functions, *Phys. Rev. Research* **2**, 023358 (2020).
- [24] M. Collura, L. Dell'Anna, T. Felser, and S. Montangero, On the descriptive power of neural-networks as constrained tensor networks with exponentially large bond dimension, *SciPost Phys. Core* **4**, 001 (2021).
- [25] F. Becca and S. Sorella, *Monte Carlo Sampling and Markov Chains* (Cambridge University Press, Cambridge, UK, 2017).
- [26] M. Bartholomew-Biggs, S. Brown, B. Christianson, and L. Dixon, Automatic differentiation of algorithms, *J. Comput. Appl. Math.* **124**, 171, (2000), Numerical Analysis 2000. Vol. IV: Optimization and Nonlinear Equations.
- [27] H.-J. Liao, J.-G. Liu, L. Wang, and T. Xiang, Differentiable Programming Tensor Networks, *Phys. Rev. X* **9**, 031041 (2019).
- [28] F. Mezzacapo, N. Schuch, M. Boninsegni, and J. I. Cirac, Ground-state properties of quantum many-body systems: Entangled-plaquette states and variational Monte Carlo, *New J. Phys.* **11**, 083026 (2009).
- [29] F. Mezzacapo and J. I. Cirac, Ground-state properties of the spin-1/2 antiferromagnetic Heisenberg model on the triangular lattice: A variational study based on entangled-plaquette states, *New J. Phys.* **12**, 103039 (2010).
- [30] W.-Y. Liu, S. J. Dong, Y.-J. Han, G.-C. Guo, and L. He, Gradient optimization of finite projected entangled pair states, *Phys. Rev. B* **95**, 195154 (2017).
- [31] J. Hasik, D. Poilblanc, and F. Becca, Investigation of the Néel phase of the frustrated Heisenberg antiferromagnet by differentiable symmetric tensor networks, *SciPost Phys.* **10**, 012 (2021).
- [32] R. P. Feynman and M. Cohen, Energy spectrum of the excitations in liquid helium, *Phys. Rev.* **102**, 1189 (1956).

- [33] L. F. Tocchio, F. Becca, A. Parola, and S. Sorella, Role of backflow correlations for the nonmagnetic phase of the  $t$ - $t'$  Hubbard model, *Phys. Rev. B* **78**, 041101(R) (2008).
- [34] D. Luo and B. K. Clark, Backflow Transformations via Neural Networks for Quantum Many-Body Wave Functions, *Phys. Rev. Lett.* **122**, 226401 (2019).
- [35] R. Penrose, Applications of negative dimensional tensors, in *Combinatorial Mathematics and its Applications*, edited by D. J. A. Welsh (Academic, New York, 1971), p. 221.
- [36] See Supplemental Material at <http://link.aps.org/supplemental/10.1103/PhysRevB.106.L081111> for extra details about the implementation of our method, together with other numerical results. We also discuss some properties of the MPBS Ansatz by showing how it can be recast into a sum of MPS and proving that, with an appropriate choice of the parameters, it can encode a volume law for the Entanglement Entropy.
- [37] M. B. Hastings, An area law for one-dimensional quantum systems, *J. Stat. Mech.* (2007) P08024.
- [38] K. E. Schmidt, M. A. Lee, M. H. Kalos, and G. V. Chester, Structure of the Ground State of a Fermion Fluid, *Phys. Rev. Lett.* **47**, 807 (1981).
- [39] V. Alba and P. Calabrese, Entanglement and thermodynamics after a quantum quench in integrable systems, *Proc. Natl. Acad. Sci. USA* **114**, 7947 (2017).
- [40] G. Carleo, K. Choo, D. Hofmann, J. E. T. Smith, T. Westerhout, F. Alet, E. J. Davis, S. Efthymiou, I. Glasser, S.-H. Lin, M. Mauri, G. Mazzola, C. B. Mendl, E. van Nieuwenburg, O. O'Reilly, H. Th evieniaut, G. Torlai, F. Vicentini, and A. Wietek, NetKet: A machine learning toolkit for many-body quantum systems, *SoftwareX* **10**, 100311 (2019).
- [41] NetKet, <https://github.com/netket/netket>.
- [42] F. Vicentini, D. Hofmann, A. Szab o, D. Wu, C. Roth, C. Giuliani, G. Pescia, J. Nys, V. Vargas-Calderon, N. Astrakhantsev, and G. Carleo, NetKet 3: Machine learning toolbox for many-body quantum systems, [arXiv:2112.10526](https://arxiv.org/abs/2112.10526).
- [43] J. Bradbury, R. Frostig, P. Hawkins, M. J. Johnson, C. Leary, D. Maclaurin, G. Necula, A. Paszke, J. VanderPlas, S. Wanderman-Milne, and Q. Zhang, JAX: Composable transformations of Python+NumPy programs (2018), <https://github.com/google/jax>.
- [44] J. Heek, A. Levskaya, A. Oliver, M. Ritter, B. Rondepierre, A. Steiner, and M. van Zee, Flax: A neural network library and ecosystem for JAX (2020), <https://github.com/google/flax>.
- [45] M. Lubasch, J. I. Cirac, and M.-C. Ba nuls, Algorithms for finite projected entangled pair states, *Phys. Rev. B* **90**, 064425 (2014).
- [46] D. L. Deng, X. Li, and S. Das Sarma, Quantum Entanglement in Neural Network States, *Phys. Rev. X* **7**, 021021 (2017).
- [47] D. Suess and M. Holz apfel, mpnum: A matrix product representation library for Python, *J. Open Source Software* **2**, 465 (2017).
- [48] S. Sorella, Green Function Monte Carlo with Stochastic Reconfiguration, *Phys. Rev. Lett.* **80**, 4558 (1998).
- [49] I. Glasser, N. Pancotti, M. August, I. D. Rodriguez, and J. I. Cirac, Neural-Network Quantum States, String-Bond States, and Chiral Topological States, *Phys. Rev. X* **8**, 011006 (2018).
- [50] G. Cataldi, A. Abedi, G. Magnifico, S. Notarnicola, N. Pozza, V. Giovannetti, and S. Montangero, Hilbert curve vs Hilbert space: Exploiting fractal 2D covering to increase tensor network efficiency, *Quantum* **5**, 556 (2021).
- [51] H. W. J. Bl ote and Y. Deng, Cluster Monte Carlo simulation of the transverse Ising model, *Phys. Rev. E* **66**, 066110 (2002).
- [52] W.-J. Hu, F. Becca, A. Parola, and S. Sorella, Direct evidence for a gapless  $Z_2$  spin liquid by frustrating N eel antiferromagnetism, *Phys. Rev. B* **88**, 060402(R) (2013).
- [53] L. Capriotti and S. Sorella, Spontaneous Plaquette Dimerization in the  $J_1$ - $J_2$  Heisenberg Model, *Phys. Rev. Lett.* **84**, 3173 (2000).
- [54] K. Choo, T. Neupert, and G. Carleo, Two-dimensional frustrated  $J_1$ - $J_2$  model studied with neural network quantum states, *Phys. Rev. B* **100**, 125124 (2019).
- [55] W.-Y. Liu, S. Dong, C. Wang, Y. Han, H. An, G.-C. Guo, and L. He, Gapless spin liquid ground state of the spin- $\frac{1}{2}$   $J_1$ - $J_2$  Heisenberg model on square lattices, *Phys. Rev. B* **98**, 241109(R) (2018).
- [56] L. Vanderstraeten, J. Haegeman, and F. Verstraete, Tangent-space methods for uniform matrix product states, *SciPost Phys. Lect. Notes*, 30 (2019).